Article type : Research Article

Time-evolving coupling functions for evaluating the interaction between cerebral oxyhemoglobin and arterial blood pressure with hypertension

Wenhao Li[1,2], Ming Zhang[3], Congcong Huo[1,2], Gongcheng Xu[1,2], Wei Chen[4,5], Daifa Wang[1,2*], Zengyong Li[4,5*]

[1]Key Laboratory for Biomechanics and Mechanobiology of Ministry of Education, School of Biological Science and Medical Engineering, Beihang University, 100191, Beijing, China

[2]Beijing Advanced Innovation Center for Biomedical Engineering, Beihang University, Beijing, 100083, China

[3]Interdisciplinary Division of Biomedical Engineering, Faculty of Engineering, The Hong Kong Polytechnic University, Kowloon, Hong Kong, SAR P.R. China

[4]Beijing Key Laboratory of Rehabilitation Technical Aids for Old-Age Disability, National Research Center for Rehabilitation Technical Aids, Beijing, 100176, China

[5]Key Laboratory of Rehabilitation Aids Technology and System of the Ministry of Civil Affairs, Beijing, 100176, China

Running title: Cardio-cerebral coupling in hypertension

Contact Information

*Corresponding author:

Daifa Wang

School of Biological Science and Medical Engineering, Beihang University Beijing, 100176

Email: daifa.wang@buaa.edu.cn

Zengyong Li

National Research Center for Rehabilitation Technical Aids, Beijing, 100176, P. R. China

Tel: +86-10-58122886, Email: lizengyong@nrcrta.cn

Abstract

Purposes: This study aimed to investigate the network coupling between arterial blood pressure (ABP) and changes in cerebral oxyhemoglobin concentration (Δ [O_2Hb]/Δ [HHb]) oscillations based on dynamical Bayesian inference in hypertensive subjects.

Methods: Two groups of subjects, consisting of 30 healthy (Group Control, 55.1 ± 10.6 y), and 32 hypertensive individuals (Group AH, 58.9 ± 8.7 y), participated in this study. A functional near-infrared spectroscopy system was used to measure the Δ [O_2Hb] and Δ [HHb] signals in the bilateral prefrontal cortex (LPFC/RPFC), motor cortex (LMC/RMC), and occipital lobe (LOL/ROL) during the resting state (12 min). Based on continuous wavelet analysis and coupling functions, the directed coupling strength (CS) between ABP and cerebral hemoglobin was identified and analyzed in three frequency intervals (I: 0.6–2 Hz, II: 0.145–0.6 Hz, III: 0.01–0.08 Hz). The Pearson correlations between the CS and blood pressure parameters were calculated in the hypertension group.

Results: In interval I, Group AH exhibited a significantly higher CS for the coupling from ABP to Δ [O_2Hb] than Group Control in LMC, RMC, LOL, and ROL. In interval III, the CS from ABP to Δ [O_2Hb] in LPFC, RPFC, LMC, RMC, LOL, and ROL was significantly higher in Group AH than in Group Control. For the patients with hypertension, diastolic blood pressure was negatively and pulse pressure was positively related to the CS from ABP to Δ [O_2Hb] oscillations in interval III.

Conclusions: The higher CS from ABP to Δ [O_2Hb] in interval I indicated that the components of cardiac activity in cerebral hemoglobin oscillations were more directly responsive to the changes in systematic ABP in patients with hypertension than in healthy subjects. Meanwhile, the higher CS from ABP to Δ [O_2Hb] in interval III indicated that the cerebral hemoglobin oscillations were

susceptible to changes in blood pressure in hypertensive subjects. The results may serve as evidence of impairment in cerebral autoregulation after hypertension. The Pearson correlation results showed that diastolic blood pressure and pulse pressure might be regarded as predictors of cerebral autoregulation function in patients with hypertension, and may be useful for hypertension stratification. This study provides novel insights into the interaction mechanism between ABP and cerebral hemodynamics and could help in the development of new assessment techniques for cerebral vascular disease.

Keywords: arterial blood pressure; cerebral hemodynamics; hypertension; dynamical Bayesian inference

Introduction

The regulatory response of cerebral blood flow variables to changes in blood pressure ensures that the cerebral blood flow matches the brain's metabolic demands and protects it from hypo- or hyperperfusion.[1] The ability of the brain to regulate its blood supply is termed cerebral autoregulation (CA).[2] CA is altered or impaired in patients suffering from hypertension and stroke.[2,3] However, studies have demonstrated that CA impairment is not an all-or-none status; it is graded and variable among different diseases.[4] Hypertension is the most powerful and important modifiable risk factor for stroke.[5,6] Long-term hypertension causes the cerebral arterial walls to harden and thicken.[7] It can also cause atherosclerosis or accelerate its development, and has a significant effect on brain structure and cognitive function.[8] Thus, monitoring the dynamic regulation between arterial blood pressure (ABP) and cerebral blood flow in patients with hypertension would permit a more personalized physiology-based therapy designed to reduce the risk of secondary brain damage.

Various mathematical methods have been developed for non-invasive assessment of CA in the resting state. The most commonly used method was transfer function analysis, which involving the relationship between ABP and cerebral blood flow velocity in the frequency domain. It quantifies CA in terms of three parameters, including the amplitude with which cerebral blood flow velocity changes driven by ABP (gain) as well as the timing (phase) and linearity (coherence) of this relationship.[9] Transfer function analysis treats CA as a linear process while it is well known that CA leads to a nonlinear pressure-flow interaction.[10] Besides, it assumes stationary signals while physiological signals including ABP and cerebral hemodynamics are nonstationary, particularly under pathophysiological conditions.[11] Despite the demonstration that the linear model provides an acceptable approximation, non-stationarities may render a high spread in the results.[12] By studying the time-varying nature of CA, we can better understand the nature of CA and track improvement or deterioration over time.

Continuous wavelet transform is a time-frequency analysis method that allows the identification of time-varying frequency and phase, and can express the non-stationary characteristics of hemodynamics.[13] Based on continuous wavelet transform, wavelet coherence analysis characterizes intermittent cross-correlations between two time series at multiple time scales, which makes no assumption about the stationarity of the input signals.[14] The wavelet phase coherence can reveal possible relationships by evaluating the match between the instantaneous phases of two signals.[15-17] It allows the identification of significant coherence of low-frequency components to cardiovascular signals even at low common power.[18] However, the contributions of amplitude and phase in the coupling strength cannot be distinguished by such methods, leading to concealment of the subtle interactions within the cardio-cerebral system.[19] Dynamical Bayesian inference (DBI) can identify time-varying dynamics in the presence of noise and follow the time evolution of the involved parameters.[20] This method provides a new means of characterizing the directed interaction mechanisms of interacting oscillators between the systems and manifests in terms of strength and directionality.[21] It can represent the functional contribution from each independent subsystem within a single coupling relationship.[22] DBI has already been used to investigate effective coupling interactions among different physiological indexes, such as neuronal, cardiorespiratory, and vascular regulation.[13,23-25] In our recent studies, the interaction between cerebral activity and ABP was detected and evaluated by using an effective coupling function based on DBI in patients with stroke.[26] However, information about the functional mechanism and the causality underlying the coupling interaction between cerebral hemodynamic variables and ABP in subjects with hypertension is far from comprehensive.

In the present work, we aimed to study the alteration in the effective coupling interaction between blood pressure changes and cerebral hemoglobin oscillations based on DBI by using functional near-infrared spectroscopy (fNIRS) in patients with hypertension. fNIRS is a widely used noninvasive imaging technique that can describe the cerebral hemodynamic responses by measuring changes in oxy- and deoxyhemoglobin concentrations (Δ [O_2Hb]/Δ [HHb], respectively).[27] Kainerstorfer et al. used fNIRS to measure Δ [O_2Hb] and Δ [HHb] to describe the CA and

demonstrated that autoregulation can reliably be measured noninvasively in the microvasculature with fNIRS.[28] Cerebral blood flow autoregulation can be monitored continuously with fNIRS in adult patients undergoing cardiopulmonary bypass.[29] Furthermore, a good correlation was reported between fNIRS and transcranial Doppler assessments of cerebral blood flow autoregulation in 23 patients with sepsis, and fNIRS shows promise for the continuous assessment of CA in adults.[30] Spatial mapping of dynamic autoregulation by multichannel fNIRS may serve as a powerful tool for identifying brain regions at specific risks for ischemia in various neurovascular diseases.[31]

In this study, cerebral hemoglobin parameters (Δ [O_2Hb]/Δ [HHb]) were measured in the prefrontal cortex (PFC), motor cortex (MC), and occipital lobe (OL) using multichannel fNIRS. The PFC is mainly responsible for cognitive control and advanced neural information processing functions, such as judgment and analysis.[32] The MC plays an important role in motor functions and is involved in the planning, control, and execution of voluntary movements.[33] The OL is the visual processing center of the brain and is crucial for coordinating language, motion perception, and visuospatial processing.[34] It was hypothesized that (1) hypertension may disturb the relationship between ABP and cerebral hemoglobin oscillations in the PFC, MC, and OL and (2) the degree of disturbance may be related to the magnitude of hypertension. In this study, coupling functions based on the DBI method were established to assess the relationship between ABP and cerebral hemoglobin oscillations in patients with hypertension. Furthermore, correlation analysis was used to reveal the relationship between the strength of the couplings and blood pressure. This study provides evidence for alterations in the mechanisms underlying cerebrovascular autoregulatory dynamics caused by hypertension.

Methods

Participants

Two groups of right-handed subjects were recruited in this study: 30 healthy (Group Control) and 32 hypertensive participants (Group AH). Participants were recruited from the local community. None of the participants experienced subjective memory problems and had unimpaired overall

cognitive function based on a Mini-Mental State Examination (MMSE) assessment.[35] Subjects in Group Control had no cardiovascular or neurological abnormalities. Hypertensive patients had systolic blood pressure (SBP) ≥ 140 mmHg or diastolic blood pressure (DBP) ≥ 90 mmHg. **Table 1** shows the analysis of the characteristics of the participants by one-way ANOVA. The experimental procedure was approved by the Human Ethics Committee of the National Research Center for Rehabilitation Technical Aids and was in accordance with the Helsinki Declaration of 1975 (revised in 2008). Written informed consent was obtained from the participants in the current study.

Data acquisition and preprocessing

The participants refrained from strenuous exercise and alcohol for at least 12 h before experimental testing. All subjects underwent a 12 min resting-state session of fNIRS and ABP measurements. They were seated comfortably in a chair in a silent and light-dimmed room. During the resting state session, the subjects were instructed to maintain their sitting position at a wakeful resting state while remaining as motionless as possible.

A 32-channel fNIRS device (NirSmart, Danyang Huichuang Medical Equipment Co., Ltd, China) was applied to measure the cerebral hemoglobin variables (Δ [O_2Hb] and Δ [HHb]) with two wavelengths (760 and 850 nm). The distance between the detectors and light sources was 3.0 cm. The sampling rates for signal acquisition were set to 10 Hz, and the differential path-length factor was set to 6.0. This fNIRS system was used and verified in our previous studies.[36] Thirty-two channels (16 channels on each side) were placed at the bilateral PFC (LPFC/RPFC), MC (LMC/RMC), and OL (LOL/ROL). The calibration function of the instrument and corresponding template was used to ascertain that the channels fell exactly in accordance with the international 10–10 electrode distribution system.[37] During the placement of the probes into the template, the hair of the subjects was manually parted to ensure that the probes were in direct contact with the scalp. Finally, the probe template was covered with black cloth to reduce the impact of ambient light. **Fig. 1(A)** shows the configuration of the sources, detectors, and measurement channels.

Continuous ABP signals were synchronized and recorded with the fNIRS measurement, which was monitored with a noninvasive blood pressure device (CNAP™ Monitor 500, CNSystems Medizintechnik AG, Graz, Austria). The sample frequency was 2000 Hz. This system comprises a sensor placed on the finger (second and third digit), a cuff for calibration, and a CNAP monitor (**Fig. 1(B)**). The ABP signal was fed into the platform using a DA100C amplifier for a Biopac MP160 (BIOPAC Systems Inc., USA).[38] The Biopac MP160 and CNAP™ were connected to a computer by Ethernet interfacing, and signals were acquired using the software Acknowledge, which allows data conversion into MATLAB-compatible formats (MATLAB 2016b, MathWorks, MA, USA) files. The 2000 Hz raw ABP data were initially downsampled to 10 Hz to match the time base of the fNIRS signals.

The fNIRS data were preprocessed according to the following steps. First, the first 2 min of raw fNIRS data were discarded for each subject to obtain a steady signal. Second, the signals were processed by low-pass filtering to 2 Hz (six-order Butterworth in the forward and backward directions) to improve the signal-to-noise ratio.[39] By applying the modified Beer–Lambert law,[40] the filtered optical density signals were converted to Δ [O_2Hb] and Δ [HHb].[41] Third, principal and independent component analysis methods [42-45] were separately performed on the Δ [O_2Hb] and Δ [HHb] signals to reduce physiological interference in the fNIRS measurements as follows: (1) Principal component analysis reduction was performed for each subject to reduce the data dimensionality (N=32) to a low dimensional (N=K). The number K of retained principal components (PCs) was determined according to the minimum number of PCs that retained more than 99% of the data variance.[43] (2) The reduced data for each individual was subjected into independent component analysis decomposition with the number of independent components equal to the number of retained principal components. All the components derived from the independent component analysis were visually inspected to determine the components that might be related to physiological interference and artifacts. (3) Significant independent components were extracted by confirming the power spectra and eliminating unwanted independent components. (4) The hemodynamic response was reconstructed using the retained independent components (N=K), and

then the data were restored to the original dimensions (N=32). Finally, the filtered Δ [O_2Hb] and Δ [HHb] signals for each channel were visually examined to check for movement artifacts, which were removed by moving standard deviation and cubic spline interpolation.[46]

Coupling function

In this study, the phase of the cerebral hemoglobin parameters (Δ [O_2Hb] and Δ [HHb]) and ABP oscillations were extracted by continuous wavelet transform, which can provide logarithmic frequency resolution and appropriate representation of low-frequency spectral structures.[47,48] Besides, this transformation allows direct reconstruction of any order time-derivatives of any order the component's amplitude and phase.[47] The oscillators of the Δ [O_2Hb] and Δ [HHb] signals were distinguished in three frequency intervals as follows:[49] I, 0.6–2 Hz; II, 0.145–0.6 Hz; and III, 0.01–0.08 Hz. The cerebral oxygenation oscillations in intervals I and II correspond to cardiac activity and respiratory activity, respectively.[23] The oscillations in frequency III mainly reflects hemodynamic fluctuations that originate from spontaneous cortical activity.[50,51]

The DBI of the coupling functions was used to reconstruct a stochastic differential model, where the deterministic part was allowed to be time varying.[20,21,52] The model to be inferred is described by the following stochastic differential equation:[53]

$$\dot{\phi}_1 = \omega_1 + q_1(\phi_1,\phi_2) + \xi_1(t) \quad (1)$$

$$\dot{\phi}_2 = \omega_2 + q_2(\phi_1,\phi_2) + \xi_2(t)$$

where ω_i is the parameter of the natural frequency, and $\phi_i$is the phase of oscillator i. The coupling function $q_i(\phi_i,\phi_\sigma)$ describes the influence of oscillator σ on the phase of oscillator i. The stochastic part is modeled by Gaussian white noise $\xi_i(t)$.

In this study, CS was applied to quantify the coupling amplitude. $CS_{i,\sigma}$ from the oscillator i to σ is defined as the Euclidean norm of the inferred parameters from the phase dynamics as follows:[52]

$$CS_{2,1} = \|q_1(\phi_1,\phi_2)\| = \sqrt{c_1^2 + c_3^2 + \ldots}, \quad (2)$$

$$CS_{1,2} = \|q_2(\phi_1,\phi_2)\| = \sqrt{c_2^2 + c_4^2 + \ldots},$$

where the odd inferred parameters are assigned to the base functions $q_1(\phi_1,\phi_2)$ for the coupling that the first oscillator imposes on the second ($CS_{1,2}$: 1→2), and vice versa ($CS_{2,1}$:2→1).

The coupling direction (CD) is defined as the normalization of the predominant coupling amplitude:[54]

$$CD = \frac{CS_{2,1} - CS_{1,2}}{CS_{2,1} + CS_{1,2}} \quad (3)$$

If $CD \in (0,1]$, then oscillator φ_2 drives φ_1; if $CD \in [-1,0)$, then oscillator ϕ_1 drives ϕ_2. The quantified values of the CS or the CD represent measures of the combined relationships between the oscillators. To characterize the coupling function between ABP and cerebral hemoglobin more clearly, channel-wise CS values were averaged in six regions of interest according to the distribution of fNIRS channels. Because coupling in the weak direction is usually not important, for the sake of simplicity, only the coupling in the principal direction was described.

Significance test

CS and CD were applied to quantitatively represent the directed coupling relationships between the oscillators from different physiological sources.[54,55] CS was defined to quantify the coupling amplitude and CD represents the predominant direction of the coupling function. Given the statistical properties of the signals, a nonzero CS may be detected from inferred couplings even from completely uncoupled or very weakly coupled systems. Therefore, ascertaining whether the detected CS is genuine or spurious due to the inference method is necessary. In this study, the amplitude-adjusted Fourier transform surrogate test was employed to detect the effectiveness of the results for the coupling functions in each interval.[56] With this method, a set of 100 amplitude-adjusted Fourier transform surrogates were generated for each signal by randomizing the phases of the original signal to create a new signal mimicking the original signal, but without having any phase relationship to it.[57] This method was applied for each channel, subject, and interval, thereby providing pairs of surrogate phases (ABP and fNIRS signal). These pairs were used as input for the

DBI to calculate the surrogate coupling. For each interval, if the actual value of CS was higher than 95% of the highest values obtained for this artificial unrelated surrogate distribution, then the CS value was sufficiently high to indicate a significant relationship between the signals at this frequency. Only those exhibiting a statistically significant difference compared with their corresponding surrogates were discussed.

Statistical analysis

Shapiro-Wilk test was applied to test the variance normality of distribution of the CS. In the present work, Wilcoxon signed-rank test was performed on the region-wise CS between Group Control and Group AH because of the non-normal distribution of this variable. Bonferroni's t-test was used for the inter-group pair-wise comparisons. In each frequency interval, two groups for CS comparison were designed (Group Control vs Group AH). Thus, there were inter-groups pair-wise comparisons. Therefore, the corrected statistical significance was defined as $p < 0.0167$ ($p < p_{origin}/3$). Pearson correlation coefficient test was conducted to identify the correlation between CS and blood pressure parameters (SBP/DBP/pulse pressure). Although nonparametric tests were used, box-and-whisker plots were used for the descriptive statistics to visually illustrate the significant differences in the CS between the two groups.

Results

Coupling between ABP and cerebral hemoglobin

The coupling quantities and characteristics were described using the inferred parameters. The coupling function represents the coupling from ABP to Δ [O_2Hb] oscillations. An example of the region-averaged coupling function from ABP to Δ [O_2Hb] oscillations in RMC in interval III is shown in **Fig. 2 (A)**, and correspond surrogate data is illustrated in **Fig. 2 (B).** Compared with that from the actual results, the amplitude of the coupling obtained from the surrogate data shown is negligible. The amplitude and shape of the coupling function might reveal the detailed mechanism of the directed interaction between ABP and cerebral hemodynamics.[58]

279

280 Directed region-wise CS was quantified to assess the influence of hypertension on network
281 coupling between cerebral hemoglobin variables and ABP. The results of the region-wise CS from
282 ABP to cerebral hemoglobin (ABP → Δ [O_2Hb] and ABP → Δ [HHb]) are shown in **Fig. 3-4**
283 (oscillation 1 → oscillation 2, oscillation 1 exerted influence on oscillation 2). Inter-group
284 comparisons of the frequency-specific CS between ABP and cerebral hemoglobin signals (Δ
285 [O_2Hb]/Δ [HHb]) were performed in six regions of interest (LPFC/RPFC, LMC/RMC, and
286 LOL/ROL).

287

288 In interval I, the CS from ABP to Δ [O_2Hb] was significantly higher in Group AH than in Group
289 Control in LMC (p = 0. 0007), RMC (p = 0.0008), LOL (p = 0.00001), and ROL (p = 0.00004)
290 **(Fig. 3 (A))**. For the CS from ABP to Δ [HHb], no significant difference was found between the
291 two groups **(Fig. 3 (B))**.

292

293 In interval III, the CS from ABP to Δ [O_2Hb] in Group AH was significantly higher than that in
294 Group Control in LPFC (p = 0.016), RPFC (p = 0.003), LMC (p = 0.00008), RMC (p = 0.0008),
295 LOL (p = 0.0007), and ROL (p = 0.001) **(Fig. 4 (A))**. The CS from ABP to Δ [HHb] was also
296 significantly higher in Group AH than in Group Control in LMC (p = 0.012) and RMC (p = 0.008)
297 (**Fig. 4 (B))**.

298

299 *Correlation analysis between CS and blood pressure*

300 The Pearson correlation between CS and blood pressure parameters (SBP/DBP/pulse pressure) was
301 calculated in the hypertension group. Pulse pressure is the difference between the SBP and DBP. A
302 significantly negative correlation was observed between DBP and CS (ABP → Δ [O_2Hb]) in LMC
303 (interval II: r = -0.467, p = 0.007; interval III: r = -0.468, p = 0.007) and RMC (interval II: r = -
304 0.427, p = 0.015; interval III, r = -0.440, p = 0.012). Correlation analysis also revealed that pulse
305 pressure was significantly positively correlated with the CS (ABP → Δ [O_2Hb]) in LMC (interval

II, r = 0.467, p = 0.007) and RMC (interval II: r = -0.440, p = 0.012; interval III: r = 0.440, p = 0.012).

Discussion

Regulation of the cerebral circulation relies on the complex interaction among the cardiovascular, respiratory, and neurophysiological parameters.[23] Cerebral circulation may be disturbed by damage to one or more of these parameters.[59] In this study, the frequency-specific coupling interaction between ABP and cerebral hemoglobin oscillations measured by fNIRS was analyzed based on coupling functions and DBI in subjects with hypertension. In interval I, Group AH exhibited significantly higher CS for the coupling from ABP to Δ [O_2Hb] than Group Control in MC and OL. In interval III, the CS from ABP to Δ [O_2Hb] in PFC, MC, and OL were significantly higher in Group AH than in Group Control. Correlation analysis revealed that DBP was negatively and pulse pressure was positively related to the CS from ABP to Δ [O_2Hb] oscillations in interval III. This study demonstrated the applicability of fNIRS-based technology in evaluating the directed interaction relationship between ABP and cerebral hemodynamic oscillations in hypertensive patients.

It is widely accepted that enhanced brain activation induces intensified blood flow in the active brain regions, leading to an increase in Δ [O_2Hb] and a decrease in Δ [HHb].[60] However, the correlation between Δ [O_2Hb] and Δ [HHb] is not perfectly negatively correlated, deviating especially in the resting state.[61,62] In the present work, the CS between ABP and Δ [O_2Hb] was not always the same as the CS between ABP and Δ [HHb]. This might be explained by the fact that the [HHb] signal may be less contaminated by systemic changes than the [O_2Hb] signal.[63] A previous study also showed that the cerebral vein (containing more [HHb]) might be less reactive to blood pressure variations than the artery (containing more [O_2Hb]).[64] Therefore, the coupling between ABP and Δ [O_2Hb] was chosen for discussion in detail below.

The oscillations in interval I reflect the effects of cardiac activity.[23] Cardiac activity is the most evident source of physiological oscillations and carries most of the burden of the increase in cerebral blood flow. Frequency interval II corresponds to respiration activity, which can provide energy for physiological activities and promote blood flow through the vessels.[23] The oscillations in intervals I and II serve as pumps that drive blood through the vessels.[65] The current study found that the oscillations between ABP and cardiac activity were more strongly coupled than those of the other oscillation sources, which is consistent with the fact. In interval I, the CS from ABP to Δ [O_2Hb]/Δ [HHb] showed higher amplitudes in patients with hypertension than in Group Control. This result indicated that the components of cardiac activity in cerebral hemoglobin oscillations more directly respond to changes in systematic ABP in hypertension patients. These hypertension-related changes in the coupling pattern appear to reflect the altered regulation between the fluctuation of systematic blood pressure and the cerebral hemodynamic response originating from cardiac activity.

In the present work, the cerebral oscillations in interval III (0.01–0.08 Hz) are thought to mainly reflect hemodynamic fluctuations that originate from spontaneous cortical activity.[50,51] The brain is critically dependent on a continuous supply of blood to function. To ensure that the cerebral blood flow matches the brain's metabolic demands, cerebral blood vessels have actively respond to spontaneous or induced blood pressure fluctuations.[66-68] CA is the ability of the brain to regulate its blood supply, which reflects the ability of cerebral microvasculature to adapt to ABP changes.[69] It has the characteristics of a high-pass filter, dampening the slower frequency oscillations (< 0.1 Hz) in response to pressure changes.[10] In subjects with a disturbed CA, the brain may be excessively sensitive to fluctuations in ABP.[12]

In interval III, the coupling from ABP to Δ [O_2Hb] showed significantly higher strength in Group AH than in Group Control (**Fig. 4**). These results indicated that ABP oscillations exerted a greater influence on Δ [O_2Hb] in patients with hypertension than in healthy controls. It appears to suggest that fluctuations in ABP would result in greater transmission to the Δ [O_2Hb] signal in the brain in

patients with hypertension. This result is consistent with the literature, which indicates that even a slight change in perfusion pressure may lead to alterations in cerebral blood flow.[70] This may be explained by the fact that the cerebral arterial and vessel walls become hardened and thickened due to the long-term effects of hypertension,[7] which in turn would increase the pulsatility of the flow through the cerebral arteries.[71] Consequently, the brain tissue is particularly vulnerable to blood pressure changes. The increased CS from ABP to cerebral hemoglobin variables in Group AH in interval III supports the idea that the loss of CA could increase the transmission of pressure to the cerebral capillaries.[72,73] This result was consistent with previous studies that CA is impaired in patients with hypertension.[74,75] A previous study also suggested that hypertension might result in the pathological alteration of the vascular wall, impairment of vital hemodynamic responses regulating cerebral perfusion.[76]

At present, various methods have been used to assess CA, such as autoregulatory index, transfer function analysis, and wavelet phase coherence (WPCO).[9] To verify the validity of the data measured in our study, the WPCO method was adopted to analyze the relationships between ABP and Δ [O_2Hb]/Δ [HHb] signals in interval III (0.01–0.08 Hz). More details about the WPCO can be found in the **Supplement**. Result showed that no significant difference was found in WPCO value between normotensive and hypertensive groups in interval III. The same results have also been observed in the previous studies using autoregulatory index and transfer function analysis to evaluate the function of CA in patients with hypertension.[77-79] According to the definition, the WPCO describes the functional connectivity, but does not provide information about causality or the directed influence between ABP and cerebral oxygenation hemodynamics. To fully understand the causal relationship, the coupling function based on DBI was applied in our study. It can provide a new means of characterizing the directed interaction mechanisms of interacting oscillators between the systems and manifests in terms of strength and directionality.[21] The current results obtained by these two methods indicate that the application of the coupling function could be better to detect the changes of CA. Previous study has proved that hypertension is involved in the pathogenesis of cardio-cerebrovascular diseases, such as stroke.[76] Therefore, monitoring and

389 evaluating of CA in patients with hypertension might be helpful for early warning of cardio-
390 cerebrovascular diseases.
391
392 The frequency-specific changes in network coupling between ABP and Δ [O_2Hb] in different brain
393 suggest an alteration of the cerebral hemodynamic response in these brain regions, which might
394 affect the function of these corresponding regions. There is growing evidence that hypertension
395 contributes to both early cerebrovascular brain aging and cognitive decline.[80] A previous study also
396 reported that hypertensive individuals have impairments in cognitive function, mobility, and mood,
397 even in the absence of clinical symptoms or disease.[81] Consistent with the literature, this study
398 found that the CS from ABP to Δ [O_2Hb] increased significantly in PFC and MC in hypertensive
399 participants relative to normotensive participants, which indicates impaired CA regulation in PFC
400 and MC. These results might relate to a decline in cognitive and motor ability in patients with
401 hypertension. These results are in line with the previous observations (Hajjar et., al, 2010) that
402 hypertension is associated with impaired vasoreactivity in all cortical brain regions and is more
403 prominent in the frontal and parietal areas.[82] Previous studies have demonstrated that patients with
404 hypertension had worse visuospatial abilities.[83] Consistent with the literature, this research found
405 that the effects that change in ABP have an increased influence on the Δ [O_2Hb] in OL.
406
407 SBP and DBP are two fundamental components of blood pressure, and both are the risk factors for
408 cardiovascular disease.[84] It has been confirmed that both SBP and DBP are important predictors of
409 brain structure and function, and the combined prediction afforded by SBP and DBP is stronger
410 than the prediction afforded by either of the two alone.[85] Pulse pressure is an indirect marker of
411 arterial stiffness, which is influenced by stroke volume and vascular resistance.[80,86] The 2018
412 European blood pressure guidelines affirmed that a pulse pressure > 60 mmHg in older
413 hypertensive persons increases the risk of cardiovascular disease.[87] Besides, it is also recognized
414 that pulse pressure is associated with brain structure and function, and suboptimal pulse pressure
415 control may increase the risk of the development of cognitive impairment in elderly individuals.[88]
416 Kannel et., al found that the incidence of cardiovascular events increased with a decrease in DBP <

80 mmHg when the SBP remained ≥ 140 mmHg.[89] Besides, a study suggests that there is an interaction between DBP and CA in elderly patients with hypertension.[90] Consistent with these studies, in interval III, DBP was negatively and pulse pressure was positively related to the CS from ABP to Δ [O_2Hb] oscillations in patients with hypertension. The results indicated that both DBP and pulse pressure are closely related to the CA function. Thus, DBP and pulse pressure might be regarded as predictors of CA function in patients with hypertension; moreover, they may be useful for hypertension stratification and permit more personalized antihypertensive therapy.

Conclusions

In this study, the frequency-specific effective interaction between ABP and cerebral hemoglobin signals (Δ [O_2Hb] and Δ [HHb]) was calculated based on coupling functions and DBI by using fNIRS in subjects with hypertension. The CS values enabled us to quantitatively describe the directed interactive regulation mechanism between ABP and cerebral hemodynamics. In interval I, Group AH showed significantly higher CS for the coupling from ABP to Δ [O_2Hb] than Group Control in LPFC, MC, and OL. In interval III, the CS from ABP to Δ [O_2Hb] in PFC, MC, and OL was significantly higher in Group AH than in Group Control, which suggests a greater influence is exerted by ABP fluctuations on cerebral hemoglobin variables in hypertension. This result indicates more direct changes in cerebral hemodynamics due to the changes in systemic blood pressure. Taken together, the hypertension-related changes in the coupling interactions might suggest an abnormal autoregulation function between ABP and cerebral hemodynamics, which might lead to the brain becoming at risk for hyper or hypoperfusion injury. The Pearson correlations showed that DBP and pulse pressure might be regarded as predictors of CA function in patients with hypertension and may be useful for hypertension stratification. Assessing the frequency-specific coupling interaction between ABP and cerebral hemodynamics based on fNIRS could provide valuable diagnostic information and help develop novel techniques to estimate the interactive autoregulation capacity in patients with hypertension.

Conflicts of interest

W.DF has a financial interest in Huichuang, Inc., which did not support this study. W.DF declare no potential non-financial competing interests. The other authors declare no potential conflict of interest.

Funding

The project was supported by the National Key Research and Development Project (2020YFC2004200), National Natural Science Foundation of China (NSFC Nos. 31771071, 61761166007, 11732015, 61675013), Fundamental Research Funds for Central Public Welfare Research Institutes (118009001000160001) and Beijing Municipal Science Technology Project (No. 161100001016013).

Author contributions statement

Conceived and designed the experiments: L.WH, H.CC. Performed the experiments: L.WH, H.CC, C.W. Analyzed the data: L.WH, X.GC. Writing review &editing: Z.M, W.DF. Supervision: L.ZY.

References

1. Kainerstorfer JM, Sassaroli A, Tgavalekos KT, Fantini S. Cerebral autoregulation in the microvasculature measured with near-infrared spectroscopy. *Journal of Cerebral Blood Flow & Metabolism.* 2015;35(6):959-966.
2. Xiong L, Liu X, Shang T, et al. Impaired cerebral autoregulation: measurement and application to stroke. *Journal of Neurology, Neurosurgery & Psychiatry.* 2017;88(6):520-531.
3. Rowley AB, Payne SJ, Tachtsidis I, et al. Synchronization between arterial blood pressure and cerebral oxyhaemoglobin concentration investigated by wavelet cross-correlation. *Physiological Measurement.* 2007;28(2):161.
4. Madureira J, Castro P, Azevedo E. Demographic and systemic hemodynamic influences in mechanisms of cerebrovascular regulation in healthy adults. *Journal of Stroke Cerebrovascular Diseases.* 2017;26(3):500-508.
5. Nadia A, Imtiaz B, Arshia A, Ejaz Ahmed V, Bashir Ahmed S. Risk factors in various subtypes of ischemic stroke according to TOAST criteria. *Journal of the College of Physicians.* 2011;21(5):280-283.
6. Veglio F, Paglieri C, Rabbia F, Bisbocci D, Bergui M, Cerrato P. Hypertension and cerebrovascular damage. *Atherosclerosis.* 2009;205(2):331-341.
7. Zuo H, Yun L, Wang J, Deng L, Su J. Relationship between four blood pressure indexes and ischemic stroke in patients with uncontrolled hypertension. *Journal of the American College of Cardiology.* 2014;64(16):C96-C96.
8. Reitz C, Tang M, J, Mayeux R, Luchsinger. Hypertension and the risk of mild cognitive impairment. *Archives of Neurology.* 2007;64(12):1734-1740.
9. Liu X, Czosnyka M, Donnelly J, et al. Comparison of frequency and time domain methods of assessment of cerebral autoregulation in traumatic brain injury. *Journal of Cerebral Blood Flow & Metabolism.* 2015;35(2):248-256.
10. Hu K, Lo M-T, Peng C-K, Liu Y, Novak V. A Nonlinear Dynamic Approach Reveals a Long-Term Stroke Effect on Cerebral Blood Flow Regulation at Multiple Time Scales. *PLoS Computational Biology.* 2012;8(7):e1002601.
11. Panerai RB. Nonstationarity of dynamic cerebral autoregulation. *Medical Engineering & Physics.* 2014;36(5):576-584.
12. Meel-van den Abeelen, S. AS, van Beek AHEA, Slump CH, Panerai RB, Claassen JAHR. Transfer function analysis for the assessment of cerebral autoregulation using spontaneous

oscillations in blood pressure and cerebral blood flow. *Medical Engineering & Physics.* 2014;36(5):563-575.

13. Ticcinelli V, Stankovski T, Iatsenko D, et al. Coherence and Coupling Functions Reveal Microvascular Impairment in Treated Hypertension. *Frontiers in Physiology.* 2017;8(749).
14. Tian F, Tarumi T, Liu H, Zhang R, Chalak L. Wavelet coherence analysis of dynamic cerebral autoregulation in neonatal hypoxic–ischemic encephalopathy. *Neuroimage Clinical.* 2016;11(C):124-132.
15. Cui R, Zhang M, Li Z, et al. Wavelet coherence analysis of spontaneous oscillations in cerebral tissue oxyhemoglobin concentrations and arterial blood pressure in elderly subjects. *Microvascular Research.* 2014;93:14-20.
16. Sheppard LW, Stefanovska A, Mcclintock PV. Testing for time-localized coherence in bivariate data. *Physical Review E Statistical Nonlinear & Soft Matter Physics.* 2012;85(4 Pt 2):046205.
17. Vermeij A, As MDA, Kessels RP, van Beek AH, Claassen JA. Very-low-frequency oscillations of cerebral hemodynamics and blood pressure are affected by aging and cognitive load. *Neuroimage.* 2014;85(1):608-615.
18. Bernjak A, Stefanovska A, Mcclintock PVE, Owen-Lynch PJ, Clarkson PBM. Coherence between fluctuations in blood flow and oxygen saturation. *Fluctuation and Noise Letters.* 2012;11(01):1240013.
19. Xie L, Li M, Dang S, et al. Impaired cardiorespiratory coupling in young normotensives with a family history of hypertension. *Journal ofHypertension.* 2018;36(11):2157-2167.
20. Stankovski T, Duggento A, Mcclintock PVE, Stefanovska A. A tutorial on time-evolving dynamical Bayesian inference. *European Physical Journal Special Topics.* 2014;223(13):2685-2703.
21. Stankovski T, Pereira T, Mcclintock PVE, Stefanovska A. Coupling functions: Universal insights into dynamical interaction mechanisms. *Reviews of Modern Physics.* 2017;89(4):045001.
22. Kralemann B, Fruhwirth M, Pikovsky A, et al. In vivo cardiac phase response curve elucidates human respiratory heart rate variability. *Nature communications.* 2013;4:2418.
23. Shiogai Y, Stefanovska A, McClintock PV. Nonlinear dynamics of cardiovascular ageing. *Physics Reports.* 2010;488(2-3):51-110.

24. Iatsenko D, Bernjak A, Stankovski T, et al. Evolution of cardiorespiratory interactions with age. *Philosophical Transactions of the Royal Society.* 2013;371(1997).
25. Schulz S, Voss A. Cardiovascular and cardiorespiratory coupling analyses: A review. *Philosophical Transactions of the Royal Society A: Mathematical, Physical and Engineering Sciences.* 2013;371(1997):20120191.
26. Su H, Huo C, Wang B, et al. Alterations in the coupling functions between cerebral oxyhaemoglobin and arterial blood pressure signals in post-stroke subjects. *PLoS ONE.* 2018;13(4):e0195936.
27. Scholkmann F, Kleiser S, Metz AJ, et al. A review on continuous wave functional near-infrared spectroscopy and imaging instrumentation and methodology. *Neuroimage.* 2014;85(Pt 1):6-27.
28. Kainerstorfer JM, Sassaroli A, Tgavalekos KT, Fantini S. Cerebral autoregulation in the microvasculature measured with near-infrared spectroscopy. *Journal of Cerebral Blood Flow & Metabolism.* 2015;35(6):959-966.
29. Brady K, Joshi B, Zweifel C, et al. Real-time continuous monitoring of cerebral blood flow autoregulation using near-infrared spectroscopy in patients undergoing cardiopulmonary bypass. *Stroke.* 2010;41(9):1951-1956.
30. Steiner LA, Pfister D, Strebel SP, Radolovich D, Smielewski P, Czosnyka M. Near-infrared spectroscopy can monitor dynamic cerebral autoregulation in adults. *Neurocritical Care.* 2009;10(1):122.
31. Reinhard M, Schumacher FK, Rutsch S, et al. Spatial mapping of dynamic cerebral autoregulation by multichannel near-infrared spectroscopy in high-grade carotid artery disease. *Journal of biomedical optics.* 2014;19(9):097005.
32. Miller EK, Cohen JD. An integrative theory of prefrontal cortex function. *Annual review of neuroscience.* 2001;24:167-202.
33. Astafiev SV, Stanley CM, Shulman GL, Corbetta M. Extrastriate body area in human occipital cortex responds to the performance of motor actions. *Nature Neuroscience.* 2004;7(5):542-548.
34. Raymond S, John S, Coleman MR, Pickard JD, David M, Ed B. Neurophysiological architecture of functional magnetic resonance images of human brain. *Cerebral Cortex.* 2005;15(9):387-413.

35. Folstein MF, Folstein SE, Mchugh PR. "Mini-mental state". A practical method for grading the cognitive state of patients for the clinician. *Journal of Psychiatric Research.* 1975;12(3):189-198.
36. Huo C, Li X, Jing J, et al. Median Nerve Electrical Stimulation–Induced Changes in Effective Connectivity in Patients With Stroke as Assessed With Functional Near-Infrared Spectroscopy. *Neurorehabilitation neural repair.* 2019:1545968319875952.
37. Oostenveld R, Peter P. The five percent electrode system for high-resolution EEG and ERP measurements. *Clinical Neurophysiology.* 2001;112(4):713-720.
38. Sharma P, Mavai M, Bhagat OL, Murugesh M, Sircar S. Slow Deep Breathing Increases Pain-tolerance and Modulates Cardiac Autonomic Nervous System. *Indian Journal of Physiology & Pharmacology.* 2017;61(2):107-113.
39. Li Z, Zhang M, Cui R, et al. Wavelet coherence analysis of prefrontal oxygenation signals in elderly subjects with hypertension. *Physiological Measurement.* 2014;35(5):777-791.
40. Khan RA, Naseer N, Qureshi NK, Noori FM, Nazeer H, Khan MU. fNIRS-based Neurorobotic Interface for gait rehabilitation. *Journal of Neuroengineering & Rehabilitation.* 2018;15(1):7.
41. Holper L, Scholkmann F, Wolf M. Between-brain connectivity during imitation measured by fNIRS. *Neuroimage.* 2012;63(1):212-222.
42. Virtanen J, Noponen TEJ, Meriläinen P. Comparison of principal and independent component analysis in removing extracerebral interference from near-infrared spectroscopy signals. *Journal of biomedical optics.* 2009;14(5):1-10, 10.
43. Zhang H, Zhang YJ, Lu CM, Ma SY, Zang YF, Zhu CZ. Functional connectivity as revealed by independent component analysis of resting-state fNIRS measurements. *Neuroimage.* 2010;51(3):1150-1161.
44. Santosa H, Hong MJ, Kim SP, Hong KS. Noise reduction in functional near-infrared spectroscopy signals by independent component analysis. *Review of Scientific Instruments.* 2013;84(7):073106.
45. Medvedev AV, Kainerstorfer J, Borisov SV, Barbour RL, VanMeter J. Event-related fast optical signal in a rapid object recognition task: improving detection by the independent component analysis. *Brain research.* 2008;1236:145-158.
46. F S, S S, T M, M W. How to detect and reduce movement artifacts in near-infrared imaging using moving standard deviation and spline interpolation. *Physiological measurement.* 2010;31(5):649.

47. Iatsenko D, McClintock PV, Stefanovska A. Linear and synchrosqueezed time–frequency representations revisited: Overview, standards of use, resolution, reconstruction, concentration, and algorithms. *Digital Signal Processing.* 2015;42:1-26.
48. Daubechies I. The wavelet transform, time-frequency localization and signal analysis. *IEEE Transactions on Information Theory.* 1990;36(5):961-1005.
49. Shiogai Y, Stefanovska A, Mcclintock PV. Nonlinear dynamics of cardiovascular ageing. *Physics Reports.* 2010;488(2-3):51.
50. Sasai S, Homae F, Watanabe H, et al. A NIRS–fMRI study of resting state network. *Neuroimage.* 2012;63(1):179-193.
51. Sasai S, Homae F, Watanabe H, Taga G. Frequency-specific functional connectivity in the brain during resting state revealed by NIRS. *Neuroimage.* 2011;56(1):252-257.
52. Andrea D, Tomislav S, Mcclintock PVE, Aneta S. Dynamical Bayesian inference of time-evolving interactions: from a pair of coupled oscillators to networks of oscillators. *Physical Review E.* 2012;86(6):061126.
53. Hagos Z, Stankovski T, Newman J, Pereira T, McClintock PV, Stefanovska A. Synchronization transitions caused by time-varying coupling functions. *Philosophical Transactions of the Royal Society A: Mathematical, Physical and Engineering Sciences.* 2019;377(2160):20190275.
54. Rosenblum MG, Pikovsky AS. Detecting direction of coupling in interacting oscillators. *Physical Review E.* 2001;64(2):045202.
55. Stankovski T, Ticcinelli V, McClintock PV, Stefanovska A. Coupling functions in networks of oscillators. *New Journal of Physics.* 2015;17(3):035002.
56. Kvandal P, Sheppard L, Landsverk SA, Stefanovska A, Kirkeboen KA. Impaired cerebrovascular reactivity after acute traumatic brain injury can be detected by wavelet phase coherence analysis of the intracranial and arterial blood pressure signals. *Journal of clinical monitoring and computing.* 2013;27(4):375-383.
57. Lancaster G, Iatsenko D, Pidde A, Ticcinelli V, Stefanovska A. Surrogate data for hypothesis testing of physical systems. *Physics Reports.* 2018;748:1-60.
58. Clemson P, Lancaster G, Stefanovska A. Reconstructing Time-Dependent Dynamics. *Proceedings of the IEEE.* 2016;104(2):223-241.
59. Donnelly J, Budohoski KP, Smielewski P, Czosnyka M. Regulation of the cerebral circulation: bedside assessment and clinical implications. *Critical care (London, England).* 2016;20(1):129-129.

60. Herold F, Wiegel P, Scholkmann F, Thiers A, Hamacher D, Schega L. Functional near-infrared spectroscopy in movement science: a systematic review on cortical activity in postural and walking tasks. *Neurophotonics.* 2017;4(4):041403.
61. Cui X, Bray S, Reiss AL. Functional near infrared spectroscopy (NIRS) signal improvement based on negative correlation between oxygenated and deoxygenated hemoglobin dynamics. *NeuroImage.* 2010;49(4):3039-3046.
62. Hoshi Y. Hemodynamic signals in fNIRS. In: *Progress in brain research.* Vol 225. Elsevier; 2016:153-179.
63. Tachtsidis I, Scholkmann F. False positives and false negatives in functional near-infrared spectroscopy: issues, challenges, and the way forward. *Neurophotonics.* 2016;3(3):030401.
64. Cheng R, Shang Y, Hayes D, Saha SP, Yu G. Noninvasive optical evaluation of spontaneous low frequency oscillations in cerebral hemodynamics. *NeuroImage.* 2012;62(3):1445-1454.
65. Li Z, Zhang M, Xin Q, et al. Age-Related Changes in Spontaneous Oscillations Assessed by Wavelet Transform of Cerebral Oxygenation and Arterial Blood Pressure Signals. *Journal of Cerebral Blood Flow & Metabolism.* 2013;33(5):692-699.
66. Petersen NH, Santiago OG, Andrés R, Arjun M, Amy H, Marshall RS. Dynamic cerebral autoregulation is transiently impaired for one week after large-vessel acute ischemic stroke. *Cerebrovascular Diseases.* 2015;39(2):144-150.
67. Paulson OB, Strandgaard S, Edvinsson L. Cerebral autoregulation. *Acta Neuropsychiatrica.* 2008;20(5):161-192.
68. H Petersen N, Ortega-Gutierrez S, Reccius A, Masurkar A, Huang A, Marshall R. Dynamic Cerebral Autoregulation Is Transiently Impaired after Large-Vessel Acute Ischemic Stroke (S19.002). *Cerebrovascular diseases.* 2015;39:144-150.
69. Hu K, Peng CK, Czosnyka M, Peng Z, Novak V. Nonlinear Assessment of Cerebral Autoregulation from Spontaneous Blood Pressure and Cerebral Blood Flow Fluctuations. *Cardiovascular Engineering.* 2008;8(1):60-71.
70. Novak V, Novak P, De CJ, Le BA, Martin R, Nadeau R. Influence of respiration on heart rate and blood pressure fluctuations. *Journal of Applied Physiology.* 1993;74(2):617.
71. Serrador JM, Sorond FA, Vyas M, Gagnon M, Iloputaife ID, Lipsitz LA. Cerebral pressure-flow relations in hypertensive elderly humans: transfer gain in different frequency domains. *Journal of Applied Physiology.* 2005;98(1):151-159.

72. Aries MJH, Elting JW, De Keyser J, Kremer BPH, Vroomen PCAJ. Cerebral autoregulation in stroke: a review of transcranial Doppler studies. *Stroke.* 2010;41(11):2697-2704.
73. Panerai RB. Cerebral Autoregulation: From Models to Clinical Applications. *Cardiovascular Engineering An International Journal.* 2008;8(1):42-59.
74. Shekhar S, Liu R, K Travis O, Roman R, Fan F. Cerebral Autoregulation in Hypertension and Ischemic Stroke: A Mini Review. *Journal of pharmaceutical sciences and experimental pharmacology.* 2017;1:21-27.
75. Immink R, van den Born B-J, Montfrans G, Koopmans R, Karemaker J, Van Lieshout J. Impaired Cerebral Autoregulation in Patients With Malignant Hypertension. *Circulation.* 2004;110:2241-2245.
76. Faraco G, Iadecola C. Hypertension: a harbinger of stroke and dementia. *Hypertension.* 2013;62(5):810-817.
77. Eames PJ, Blake MJ, Panerai RB, Potter JF. Cerebral autoregulation indicesare unimpaired by hypertensionin middle aged and older people. *American Journal of Hypertension.* 2003;16(9):746-753.
78. Serrador J, Sorond F, Vyas M, Gagnon M, Iloputaife I, Lipsitz L. Cerebral pressure-flow relations in hypertensive elderly humans: Transfer gain in different frequency domains. *Journal of applied physiology (Bethesda, Md : 1985).* 2005;98:151-159.
79. Zhang R, Witkowski S, Fu Q, Claassen JA, Levine BD. Cerebral hemodynamics after short- and long-term reduction in blood pressure in mild and moderate hypertension. *Hypertension.* 2007;49(5):1149-1155.
80. Gąsecki D, Kwarciany M, Nyka W, Narkiewicz K. Hypertension, brain damage and cognitive decline. *Curr Hypertens Rep.* 2013;15(6):547-558.
81. Hajjar I, Yang F, Sorond F, et al. A novel aging phenotype of slow gait, impaired executive function, and depressive symptoms: relationship to blood pressure and other cardiovascular risks. *The journals of gerontology Series A, Biological sciences and medical sciences.* 2009;64(9):994-1001.
82. Hajjar I, Zhao P, Alsop D, Novak V. Hypertension and cerebral vasoreactivity: a continuous arterial spin labeling magnetic resonance imaging study. *Hypertension.* 2010;56(5):859-864.

83. Muela H, Costa‐Hong V, Yassuda M, et al. Hypertension Severity Is Associated With Impaired Cognitive Performance. *Journal of the American Heart Association.* 2017;6:e004579.
84. Sesso HD, Stampfer MJ, Rosner B, et al. Systolic and Diastolic Blood Pressure, Pulse Pressure, and Mean Arterial Pressure as Predictors of Cardiovascular Disease Risk in Men. *Hypertension.* 2000;36(5):801-807.
85. Elias M, Torres R, Davey A. Diastolic Blood Pressure, Not Just Systolic Blood Pressure, Is Related to Cerebral Measures in Middle Age: Implications for Prospective Studies. *American journal of hypertension.* 2018;31.
86. Dart AM. Should pulse pressure influence prescribing? *Australian prescriber.* 2017;40(1):26-29.
87. Williams B, Mancia G, Spiering W, et al. 2018 ESC/ESH Guidelines for the management of arterial hypertension. *Kardiologia polska.* 2019;77(2):71-159.
88. Wong B, Chaturvedi N, Tillin T, et al. Increased pulse pressure associated with a decline in brain structure and function: the Southall and Brent revisited (Sabre) study. *Journal of Hypertension.* 2019;37:e218-e219.
89. Kannel WB, Wilson PWF, Nam B-H, D'Agostino RB, Li J. A likely explanation for the J-curve of blood pressure cardiovascular risk. *The American Journal of Cardiology.* 2004;94(3):380-384.
90. Vishram JK, Borglykke A, Andreasen AH, et al. Impact of age on the importance of systolic and diastolic blood pressures for stroke risk: the MOnica, Risk, Genetics, Archiving, and Monograph (MORGAM) Project. *Hypertension.* 2012;60(5):1117-1123.

Figure 1. Schematic of the experimental layout. (A) Channel configuration of the fNIRS layout with 20 sources (blue) and 12 detectors (yellow), resulting in 32 channels. ‘‘C’’ means channel. Six cerebral cortex areas are separated by the rectangular frame as LPFC, RPFC, LMC, RMC, LOL, and ROL. (B) Location illustration of the ABP layout.

Figure 2. An example of region-averaged coupling functions in interval III. (A) The coupling function describes the functional influence from the ABP to Δ [O_2Hb] oscillator in RMC. (B) The corresponding surrogate coupling function. represents Δ [O_2Hb] oscillations and represents ABP oscillations.

Figure 3. Comparison of the region-wise CS between different groups in interval I from ABP to (A) Δ [O_2Hb] and (B) Δ [HHb]. The arrows represent direction. ‘‘*’’ indicates a significant difference. Control: Group Control; AH: Group AH.

Figure 4. Comparison of region-wise CS between different groups in interval III from ABP to (A) Δ [O_2Hb] and (B) Δ [HHb]. The arrows represent direction. ‘‘*’’ indicates a significant difference. Control: Group Control; AH: Group AH.

Table 1. Characteristics of the participants

Parameters	Group Control (N=30)	Group AH (N=32)	*p* value
Age (years)	55.1 ± 10.6	58.9 ± 8.7	0.133
Sex (male/female)	16/14	18/14	0.821
BMI	25.7 ± 3.3	25.8 ± 3.5	0.909
MMSE	25.7 ± 2.3	25.9 ± 1.9	0.796
Systolic blood pressure (mmHg)	126.2 ± 11.2	150.9 ± 16.1	< 0.000*
Diastolic blood pressure (mmHg)	82.6 ± 6.5	89.9 ± 0.8	0.003*

Values are presented as means with standard deviations. BMI, Body Mass Index. *p* for the difference between Group Control and Group AH. *$p < 0.05$.

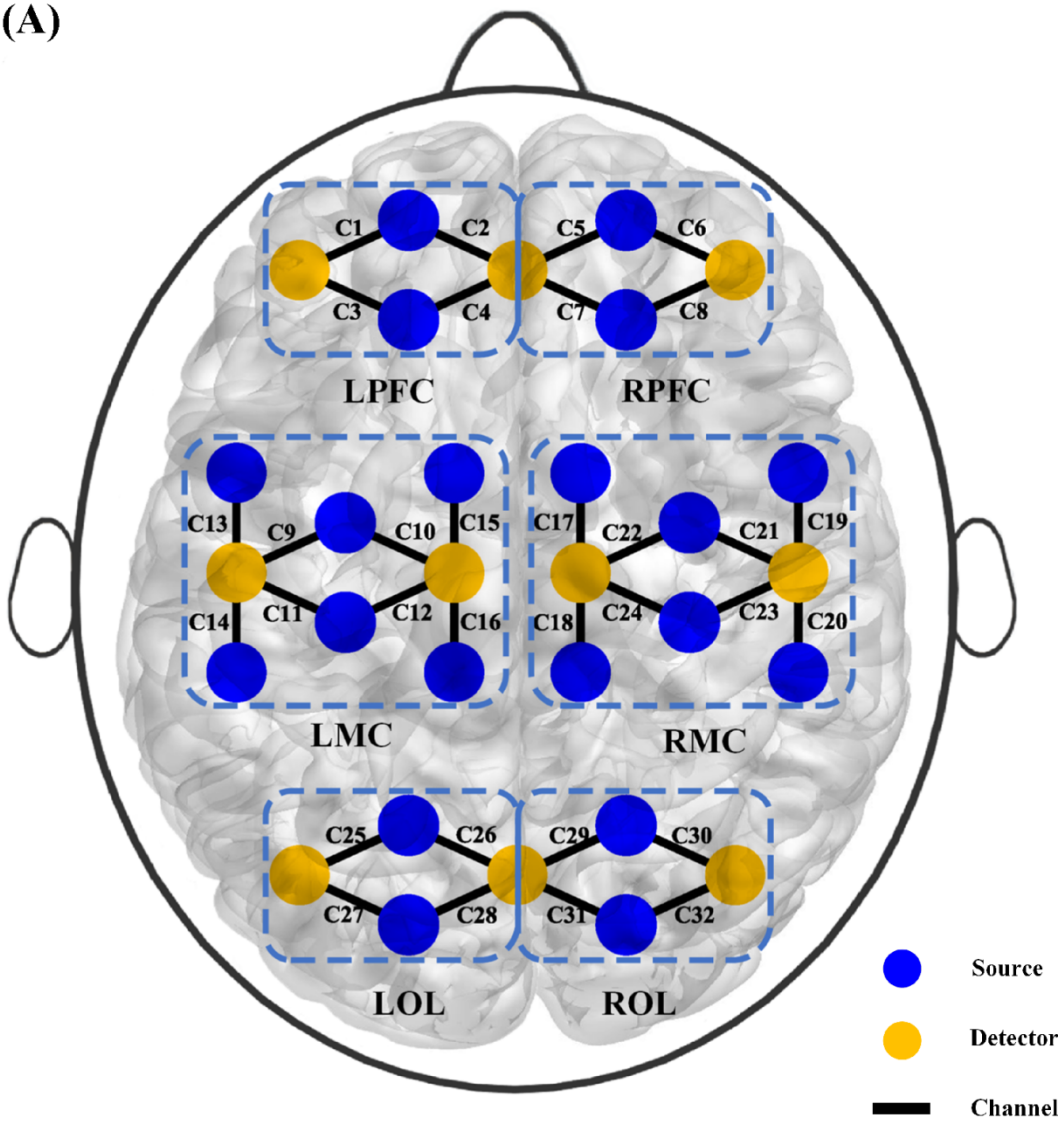

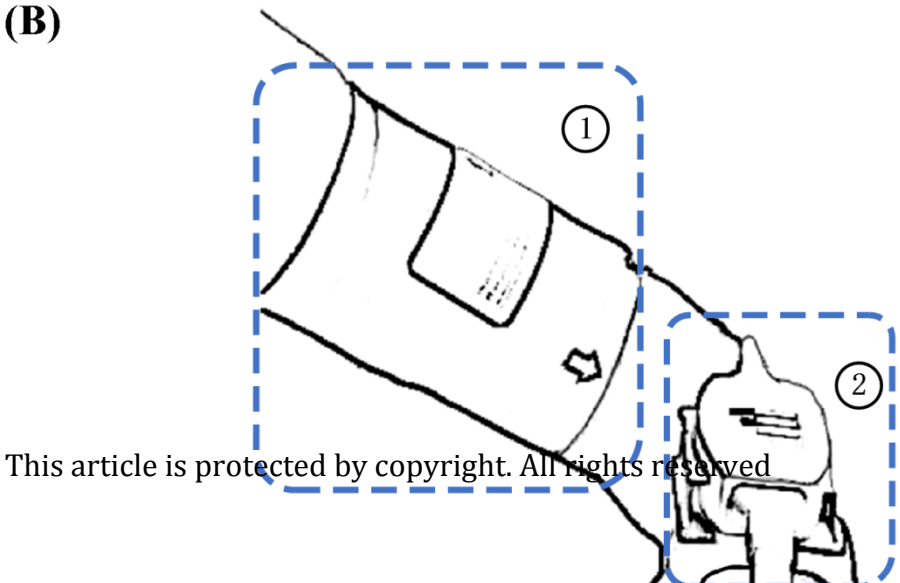

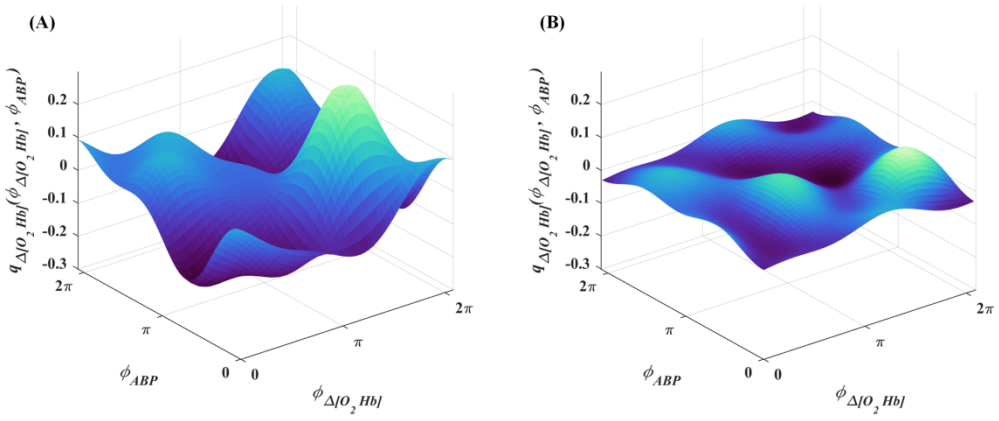

mp_14627_f2.tif

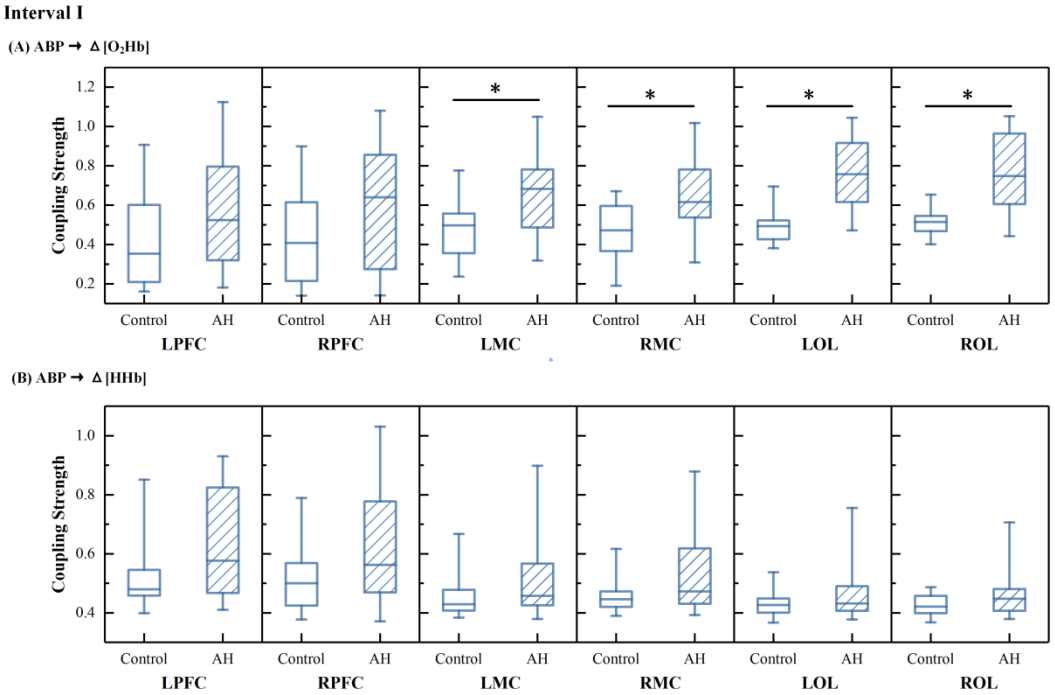

mp_14627_f3.tif

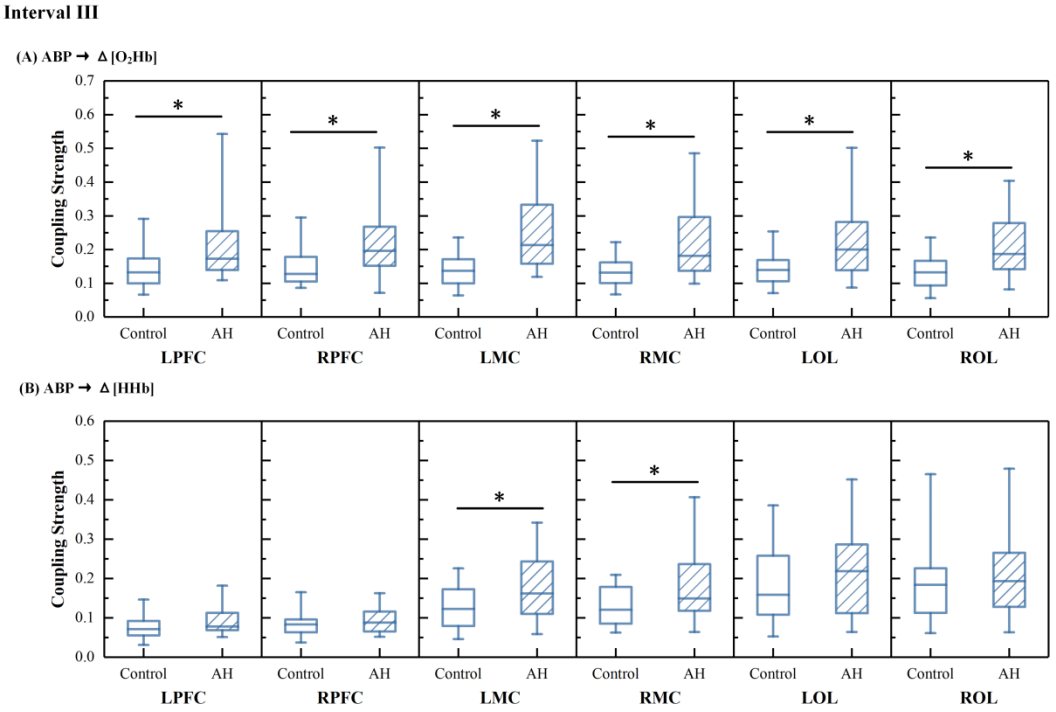

mp_14627_f4.tif